Available online at www.sciencedirect.com
ScienceDirect
Carbohydrate Polymers 71 (2008) 235–244
Carbohydrate Polymers
www.elsevier.com/locate/carbpol

Morphology and barrier properties of solvent cast composites of thermoplastic biopolymers and purified cellulose fibers

M.D. Sanchez-Garcia [a], E. Gimenez [b], J.M. Lagaron [a,*]

[a] *Novel Materials and Nanotechnology, IATA, CSIC, Apdo. Correos 73, 46100 Burjassot, Spain*
[b] *Area of Materials, Department of Industrial Systems Engineering and Design, University Jaume I, 12071 Castellón, Spain*

Received 12 March 2007; received in revised form 23 May 2007; accepted 24 May 2007
Available online 12 June 2007

Abstract

This paper shows and discusses the morphology, thermal and transport properties of solvent cast biocomposites of poly(lactic acid) (PLA), polyhydroxybutyrate-co-valerate (PHBV) and polycaprolactones (PCL) containing purified alfa micro-cellulose fibers as a function of filler content. The SEM, optical microscopy and Raman imaging results indicate that a good dispersion of the fibers in the matrix was achieved for the three biopolymers. However, detrimental fiber agglomeration was clearly observed to take place for samples with fiber contents in excess of 5 wt%. The heat of fusion (related to crystallinity) of the semicrystalline PCL and PHBV biopolymers was seen to decrease, particularly in low fiber content biocomposites, but it seemed to increase slightly in the highly amorphous PLA biocomposites. In accordance with the morphology data, water and D-limonene direct permeability were seen to decrease to a significant extent in the biocomposites with low fiber contents. The permeability reduction was mostly related to a decrease in diffusivity but solubility was also found to be favorable. The main conclusion from this work is that purified cellulose fibers can also be used to enhance the barrier properties of thermoplastic biopolyesters of interest in, for instance, packaging and membrane applications.

Keywords: Cellulose fibers; Composites; Barrier properties; PLA; PCL and PHBV

1. Introduction

There is a growing worldwide interest pushed by governments and societies to increment the responsible use of renewable resources in commodity plastic products in order to reduce the waste associated to their use, particularly in packaging applications (Petersen et al., 1999; Haugaard et al., 2001). The use of biodegradable plastics and resources are seen as one of the many strategies to minimise the environmental impact of petroleum-based plastics. The biological base of these new biopolymers provides a unique opportunity to incorporate a highly demanded property of these materials, i.e. the compostability. It must be considered that among the plastic waste there are products with a high degree of contamination and recycling requires a high energy cost. Therefore, compostability is a very interesting property that guarantees that these new biomaterials will degrade mostly into carbon dioxide and water after disposal (Kijchavengkul, Auras, Rubino, Ngouajio, & Fernandez, 2006). These biodegradable materials present a number of excellent and promising properties in a number of applications, including packaging, automotive and biomedical sectors. Thus, thermoplastic biodegradable polymers, such as poly(lactic acid) (PLA), polyhydroxyalkanoate (PHA) and polycaprolactones (PCL), exhibit an excellent equilibrium of properties, i.e. they are processable using conventional plastics machinery and, for the case of the first two, they arise from renewable resources. PLA is a thermoplastic biopolyester produced from L-lactid acid, which typically comes from the fermentation of corn starch. Currently, PLA is being commercialized and being used as a food packaging polymer for short shelf-life products with common applications such as containers,

* Corresponding author.
E-mail address: lagaron@iata.csic.es (J.M. Lagaron).

0144-8617/$ - see front matter © 2007 Elsevier Ltd. All rights reserved.
doi:10.1016/j.carbpol.2007.05.041

drinking cups, sundae, and salad cups, overwrap and lamination films, and blister packages (Auras, Kale, & Singh, 2006). In PHAs (polyhydroxyalkanoates) family, the most widely used material is the polyhydroxybutyrate (PHB) and its copolymers with valerate. These microbial biopolymers are storage materials produced by a variety of bacteria in response to particular environmental stresses (Peoples & Sinskey, 1990). Polyhydroxybutyrate (PHB) is a naturally occurring β-hydroxyacid (a linear polyester). The homopolymer, poly(hydroxybutyrate) PHB, and its copolymer with hydroxyvalerate, PHBV, are biodegradable engineering thermoplastic polymers with important trade properties that make them suitable in many applications for which petroleum-based synthetic polymers are currently used. PHB polymers are already being used in small disposable products and in packaging materials (Rosa, Lotto, Lopes, & Guedes, 2004). Finally, PCL is a thermoplastic biodegradable polyester synthesized by chemical conversion of crude oil. PCL has good water, oil, solvent, and chlorine resistance, a low melting point, and low viscosity, and is easily processed using conventional melt blending technologies (Gross & Kalra, 2002). PCL is at this time being investigated for its use in biomedical utensils, pharmaceutical controlled release systems, and in biodegradable packaging (PigŁowski & Kiersnowski, 2006; Iannace, Luca, & Nicolais, 1990).

In order to tailor the properties and reduce material costs, it is often desirable to combine bioplastic materials with other, ideally, more inexpensive substances, such as natural fibers (Bodros, Pillin, Montrelay, & Baley, 2007). Reinforcement of some of these bioplastics with lignocellulosic fibers has previously been carried out with the overall aim of increasing its biodegradation rate and to enhance mechanical properties, i.e. this route led to considerable improvements in the composites tensile strength (Tserki, Matzinos, Zafeiropoulos, & Panayiotou, 2006). However, to the best of our knowledge there is not prior literature on the use of these reinforced biocomposites to modify the barrier properties of such biopolymers. Lignocellulosic materials appear to be suitable fillers or reinforcing agents for biodegradable matrices since they exhibit interesting properties such as a renewable nature, wide variety of feedstocks available throughout the world, nonfood agricultural-based economy, low energy consumption, low cost, low density, high specific strength and modulus, high sound attenuation of lignocellulosic-based composites, comparatively easy processability due to their nonabrasive nature, which allows high filling levels and significant cost savings, and finally relatively high reactive surface, which can be used for grafting specific groups (Orts et al., 2005).

Thus, the use of lignocellulosic fibers derived from annually renewable resources as a reinforcing phase in polymeric matrix composites provides positive environmental benefits with respect to ultimate disposability and raw materials use. A major disadvantage of cellulose fibers is their hydrophilic character that makes them, in principle, sparingly miscible with less polar or nonpolar polymers (Mutje, Girones, & Lopez, 2006). Therefore, to develop such biocomposites with optimum properties, it has been customary to decrease the hydrophilicity of the lignocellulosic materials by chemical modification or to promote interfacial adhesion through the use of compatibilizers (Nitz, Semke, Landers, & Mulhaupt, 2001). The chemical modification is usually obtained through the use of reagents having functional groups that are capable of bonding to the hydroxyl groups of the lignocellulosic materials (Rana, Basak, Mitra, Lawther, & Banerjee, 1997; Ichazo, Albano, Gonzalez, Perera, & Candal, 2001). Another drawback of lignocellulosic fillers is their high moisture absorption and the resulting swelling and decrease in mechanical properties (Najafi, Tajvidi, & Chaharmahli, 2006.) Moreover, the processing temperature of composites is restricted to about 200 °C because lignocellulosic materials exhibit significant degradation processes above this temperature. In spite of that, higher thermal stability, less color, more homogeneity and enhanced properties can be achieved by using highly purified alfa cellulose fibers. In the latter material, lignin and hemicellulose residues have been virtually eliminated from the natural fiber and, therefore, a more robust filler is thus generated (Malainine, Mahrouz, & Dufresne, 2004). Properties of fiber reinforced composites depend on many factors, for instance fiber/matrix adhesion, volume fraction of fiber, fiber aspect ratio, fiber orientation, and stress/transfer efficiency through the interface (Dufresne, Dupeyre, & Paillet, 2003). Fiber size and processing techniques have a significant incidence on the final properties of the composites, because they define the degree of fiber dispersion and their impact on matrix morphology. Fiber content in biodegradable polymers is also frequently associated with the degree of dispersion or agglomeration of the fibers, because high fiber contents in the matrix produce fiber agglomeration, caused by the tendency of the filler to form hydrogen bonding with each other (Tserki et al., 2006).

As mentioned above, fiber dispersion has a stronger effect in the mechanical properties of the composites, which can ultimately be reflected on other potential properties such as barrier properties. The presence of impermeable crystalline fibers is thought to increase the tortuosity or detour factor in the materials leading to slower diffusion processes and, hence, to lower permeability. To enhance barrier properties to gases and vapors the filler should be less permeable or impermeable and have optimum dispersion and a high aspect ratio (filler length/thickness ratio) (Lagaron, Catalá, & Gavara, 2004). Fiber size is also relevant because by reducing fiber size, high surface to volume ratio of the filler in the matrix is achieved, and this makes possible to strongly impact properties with low additions of the reinforcing elements without detrimental impact on other important parameters such as crystallinity, optical properties and material toughness. The literature results show that composites with a smaller particle size and good dispersion have higher properties compared to others of greater size (Khalil, Shahnaz, Ratnam, Ahmad, & Fuaad, 2006). Current technologies allow to reduce fiber cross-section

to the nanometer level as in the case of the so-called Micro Fibrillated Cellulose (MFC) (López-Rubio et al., 2007) or in electrospun cellulose fibers (Huang, Zhang, & Kotaki, 2003).

In summary, it is well known that cellulose fibers can enhance mechanical properties in as much as other synthetic fibers (Nabi Sahed & Jog, 1999), however, very little is known about their impact on barrier properties. Regarding the latter, only a previous work reported about reductions in oxygen permeability for PLA composites containing microcrystal cellulose (Petersson & Oksman, 2006). In this first study, the morphology and solvent barrier properties as a function of filler content of biocomposites of PLA, PCL and PHBV containing purified alfa cellulose fibers as reinforcing elements are presented and discussed.

2. Materials and methods

2.1. Materials

The bacterial polyhydroxyalkanoate grade was purchased to Goodfellow Cambridge Limited, UK, in pellet form. The supplied material was a melt-processable semicrystalline thermoplastic PHBV (Polyhydroxybutyrate with 12 mol% of Valerate) copolymer made by biological fermentation from renewable carbohydrate feedstocks. The PCL grade FB100 was kindly supplied in pellet form by Solvay Chemicals, Belgium. This grade has a density of 1.1 g/cm^3 and a mean molecular weight of 100,000 g/mol. The semicrystalline PLA used was a film extrusion grade manufactured by Natureworks (with a D-isomer content of approximately 2%). The molecular weight had a number–average molecular weight (M_n) of ca. 130,000 g/mol, and the weight–average molecular weight (M_w) was ca. 150,000 g/mol.

A purified cellulose fiber grade from CreaFill Fibers Corp. (US), having an average fiber length of 60 μm and an average fiber width of 20 μm was used. According to manufacturer's specifications, these fibers had an alfa-cellulose content of >99.5% and an aspect ratio of ca. 3.

2.2. Preparation of blends

Solution-cast film samples of the biodegradables materials with 1, 2, 4, 5, and 10 wt% fiber contents were prepared with a dry film thickness of around 100 μm, using chloroform as a solvent. Fiber solutions in chloroform were mixed in a homogenizer (Ultraturrax T25 basic, Ika-Werke, Germany) for 2 min and were then stirred with the polymer at 40 °C during 30 min and, subsequently, cast onto Petri dishes to generate films after solvent evaporation at room temperature conditions.

2.3. SEM measurements

For scanning electron microscopy (SEM) observation, the samples were cryofractured by hand after immersion in liquid nitrogen, mounted on bevel sample holders and sputtered with Au/Pd in a vacuum. The SEM pictures (Hitachi S4100) were taken with an accelerating voltage of 10 keV on the sample thickness.

2.4. AFM

AFM measurements were performed using a Nano-Scope IIIa (Digital Instruments Inc.) to investigate the morphology on the top and fracture surfaces of the cast films in the biocomposites. The images were scanned in tapping mode in air using commercial Si cantilevers (Digital Instruments Inc.) with a resonance frequency of 320 kHz.

2.5. Optical light polarized microscopy

Polarized light microscopy (PLM) examinations using an ECLIPSE E800-Nikon with a capture camera DXM1200F-Nikon were carried out on both sides of the cast samples. A 40× times objective was used to examine the samples.

2.6. Laser Raman Spectrophotometer

Raman images were taken with a Jasco NRS-3100 Confocal Micro-Raman spectrophotometer, which provides high laser spot lateral and depth sample resolutions, i.e. measured samples areas are smaller than 2 microns when the optimum confocal instrumental setup is selected and by using a 100× microscope objective. The laser source used was a red light tuned at 632.8 nm and powered at 12.4 mW. Raman imaging was carried out in the point by point mode by rationing the area of two Raman bands arising from the different phases of the composites, and were constructed by taken 15 × 15 spectra equally spaced across the selected sample area.

2.7. DSC measurements

Differential scanning calorimetry (DSC) of PHBV, PLA, PCL and its biocomposites were performed on a Perkin-Elmer DSC 7 thermal analysis system on typically 7 mg of dry material at a scanning speed of 10 °C/min from room temperature to the melting point using N_2 as the purging gas. Before evaluation, the thermal runs were subtracted similar runs of an empty pan. The DSC equipment was calibrated using indium as a standard and typically only one measurement was carried out on the samples.

2.8. Gravimetric measurements

Direct permeability to D(+)-limonene of 95% purity (Panreac Química, Spain) and direct permeability to water were determined from the slope of weight loss vs. time experiments at 24 °C and 40%RH. The films were sandwiched between the aluminium top (open O-ring)

and bottom (deposit for the permeant) parts of aluminium permeability cells. A Viton rubber O-ring was placed between the film and the bottom part of the cell to enhance sealability. Then the bottom part of the cell was filled with the permeant and the pinhole secured with a rubber O-ring and a screw. Finally, the cell was placed in the desired environment and the solvent weight loss through a film area of 0.001 m^2 was monitored and plotted as a function of time. The samples were preconditioned at the desired testing conditions for 24 h, and to estimate permeability we used only the liner part of the weight loss data to ensure sample steady-state conditions. Cells with aluminum films (with thickness of ca. 100 microns) were used as control samples to estimate solvent loss through the sealing. The permeability sensibility of the permeation cells was determined to be of ca. 0.01×10^{-13} kg m/s m^2 Pa based on the weight loss measurements of the aluminium cells. Cells clamping polymer films but with no solvent were used as blank samples to monitor water uptake. Solvent permeation rates were estimated from the steady-state permeation slopes. Organic vapor weight loss was calculated as the total cell loss minus the loss through the sealing and plus the water weight gain. The tests were done in duplicate.

The diffusion coefficient of D-limonene was estimated during desorption experiments at 24 °C and 40%RH by means of weight loss experiments using an analytical balance Voyager® V11140. Thus, at saturation conditions, checked by observing no changes in successive weight uptake measurements of the specimens dipped in the compound, the samples were thoroughly bottled with a tissue to remove the excess of aroma vapor condensed over the film surface (this step is considered as time zero) and were periodically weighted until they yielded constant weight. D values were obtained from fitting the experimental data vs. time to the first six sum terms of the corresponding solution of Fick's second law (1) during desorption experiments (Crank, 1975).

$$\frac{M_t}{M_e} = \frac{8}{\pi^2} \sum_{n=0}^{\infty} \frac{1}{(2n+1)^2} \exp\left\{\frac{-D(2n+1)^2\pi^2 t}{l^2}\right\} \quad (1)$$

3. Results and discussion

3.1. Biocomposites morphology

Simple naked eye examination of the films obtained by the solvent cast method applied indicated that good filler dispersion was achieved in the low fiber content materials, since optical properties such as transparency of the composites remained virtually unmodified compared to the neat biopolymers. On the other hand, cast films with fiber contents beyond 5% showed fiber agglomeration in the matrix as fiber white agglomerates could easily be spotted in the films. To observe the morphology at the micron and submicron level, SEM observations were initially carried out in the biocomposites. SEM experiments usually allow a clear observation of the phase morphology in composite materials and do additionally provide information about interfacial adhesion. The SEM results showed that observation of the biofiller strongly depended on the loading levels for all biopolymers. Fig. 1 shows the fracture morphology of some of the films prepared with low, medium and high fiber contents. The SEM examination reveals that a homogeneous distribution of the fibers in the PHBV and PCL matrixes and a continuous phase morphology must have been achieved at low fiber contents (1 wt%) since the presence of the fibers cannot be unambiguously

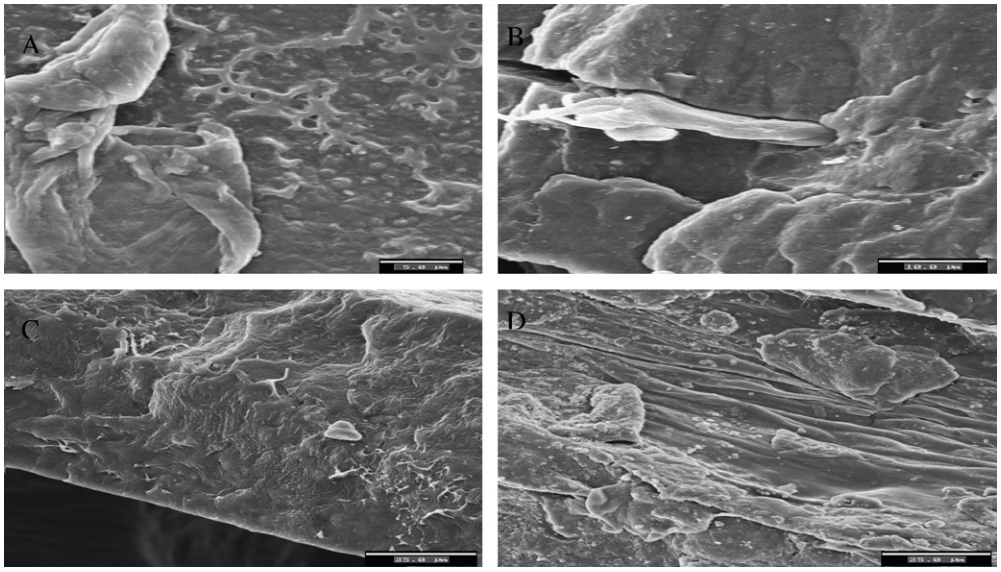

Fig. 1. Scanning electron micrographs of the cross section of: (A) A film prepared by casting of PHBV with 1 wt% fiber content (scale marker is 5 microns). (B) A film prepared by casting of PHBV with 10 wt% fiber content (scale marker is 10 microns). (C) A film prepared by casting of PCL with 1 wt% fiber content (scale marker is 25 microns). (D) A film prepared by casting of PCL with 5 wt% fiber content (scale marker is 25 microns).

discerned from the matrix (see Fig. 1A and C). On the contrary, films prepared by casting with 10 wt% fiber content in the PHBV matrix easily revealed the presence of long fibers, fiber agglomerates and phase discontinuity likely as a result of insufficient dispersion caused by self-association of excess filler (Fig. 1B). Fig. 1D indicates that for a 5 wt% fiber addiction to the PCL matrix, long fibers can be seen aligned along the facture surface.

It is evident that given the relatively large size of the fibers, the difficult observation of these must be attributed to a limitation of the SEM technique to resolve between the two components, filler and matrix, particularly when the dispersion of the filler and phase continuity seems high. AFM is a very powerful technique for the observation of materials morphology and it also provides a feasible route to investigate the topography of films containing micro- and nanofibers (Kirby, Ng, & Waldron, 2006). AFM and transmission electron microscopy (TEM) replicate techniques have previously been used to study the nanoscale surface chemistry and the morphology of biodegradable materials containing fibers when SEM observations were not successful (Kirby et al., 2006; López-Rubio et al., 2007). Consequently, additional observation of the samples was carried out by AFM at the top surface and cryofractured surfaces. Even with this technique it was not very easy to detect the fibers at the samples surface. Nevertheless, Fig. 2 shows, as an example, that the surface roughness of the composites can be well resolved by the AFM tip. This figure shows the presence on the top surface of a fiber in the 1 wt% fiber-PHBV sample prepared by casting. The picture reveals the presence of what appears to be a fiber of 50 μm in length and a width of approximately ca. 8.5 μm, which seems strongly attached to matrix. Since the typical fiber thickness of the starting filler is around 20 microns, the detected thinner fiber could suggest (see later) that fibers could split in the cross section dimension during the homogenization step in the preparation.

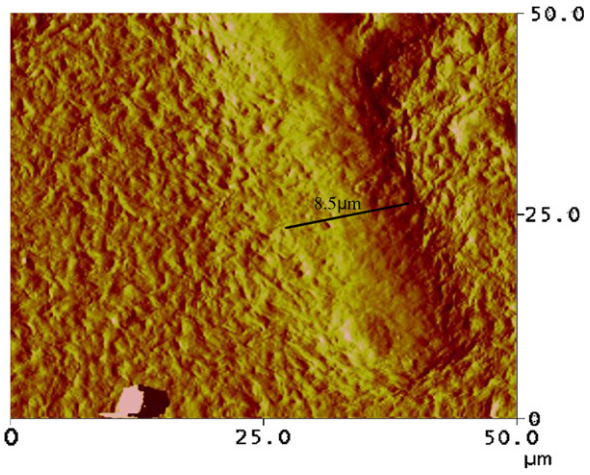

Fig. 2. Atomic force microscopy phase typical image of the top surface of a cast sample of PHBV containing 1 wt% of fibers.

However, the best techniques to resolve the morphology of the fibers in the biopolymer matrixes turned out to be in this study polarized optical microscopy (Colomb et al., 2005) and Raman imaging. Polarized optical light microscopy photographs allowed to take clear images of the cellulose fibers embedded in the biodegradable matrixes. The biocomposites showed no apparent differences in fiber homogeneity across the thickness and top and bottom sides of the biocomposites showed similar morphologies. However, some of the samples, particularly higher filler content biocomposites, showed the presence of larger fiber aggregates, probably deposited by gravity, at the bottom of the cast films. Observation of the fibers was, however, easier in the PLA samples because these particular samples were totally transparent. Fig. 3A and B clearly shows the presence of highly dispersed fibers in the 1 and 5 wt% fiber-PLA sample prepared by casting. The Fig. 3A indicates that the dimensions of the fibers in the biocomposites are not homogeneous but vary from 10 to 25 microns in thickness and between 50 and 100 microns in length. In the 5 wt% fiber-PLA sample (see Fig. 3B) it can be easily observed that the excess of fibers results in a tendency of these to crowd together and entangle. The identification of the filler in the other two biomaterials was feasible but due to a lack of transparency in the cast films, the phase structure could not be so well resolved as for the PLA case. Fig. 3C and D shows the presence of dispersed fibers in the 1 and 5 wt% fiber-PCL samples. The Figs. 3C (PCL+1 wt% fiber) and 3E (PHBV+1 wt% fiber) suggest that the cross-sectional dimensions of the fibers in these biocomposites are finer than in PLA, i.e. the observed fibers are smaller than 5 microns in thickness and with lengths around 60 microns. The reason for the latter observation is uncertain but it could be due to the specific rheological properties or interactions between the different materials and the fibers during the homogenization step. To check for the latter observation In Fig. 3D, the PCL biocomposite containing 5 wt% of fiber shows that the filler begin to collide and agglomerate, albeit this event is not as clear as was seen for PLA.

A definitive proof of the above mentioned good fiber phase dispersion and phase morphology for the 1 wt% fiber content composites was provided by the Raman chemical compositional image depicted in Fig. 4 for the case of the PLA composite. Fig. 4 highlights the various parts where signal from the fibers is stronger in the composites (green-yellowed areas). A curious observation is that, despite the fact that the confocal laser spot was much smaller (ca. 1 micron in axial resolution and 2 microns in depth) than the width of most fibers, no single spectrum of the Raman image showed the neat spectrum of the fibers within the biocomposites, whereas this was often the case when the matrix was targeted with the laser spot. This observation suggests that the fibers are well embedded in the matrix or even intercalated by the matrix.

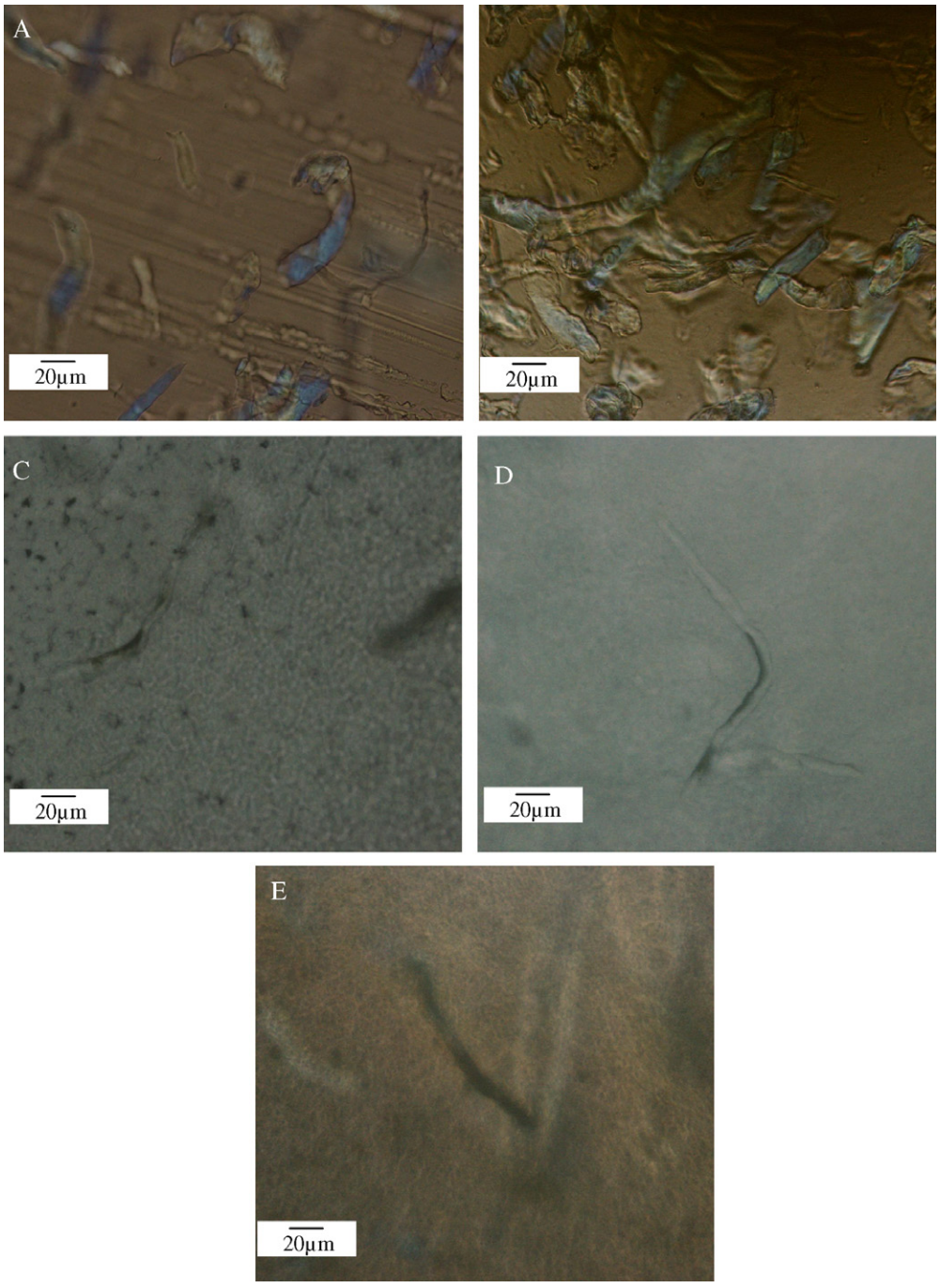

Fig. 3. Optic micrographs of: (A) A film prepared by casting of PLA with 1 wt% fiber content. (B) A film prepared by casting of PLA with 5 wt% fiber content. (C) A film prepared by casting of PCL with 1 wt% fiber content. (D) A film prepared by casting of PCL with 5 wt% fiber content. (E) A film prepared by casting of PHBV with 1 wt% fiber content.

3.2. Thermal properties

Melting temperature (T_m) and Heat of fusion (ΔH_m) corrected for biopolymer content in the biocomposites were determined from the DSC first heating runs of the samples. These are summarized in Table 1 for cast films with different fiber contents. The PHBV copolymer shows a multiple melting endotherm with two peaks, reflect of the heterogeneity in the crystalline structure of this copolymer. Table 1 shows the variation of the two thermal parameters as a function of fiber content for the PCL and PHBV composites. From this Table 1, the heat of fusion of the latter two biomaterials is seen to drop in the composites, however, this drop, and also the melting point drop in PHBV, is larger for the samples with lower fiber contents, i.e. for the samples exhibiting more dispersed filler morphologies. Higher filler dispersion and interfacial adhesion is thought to hinder to some extent polymer chains

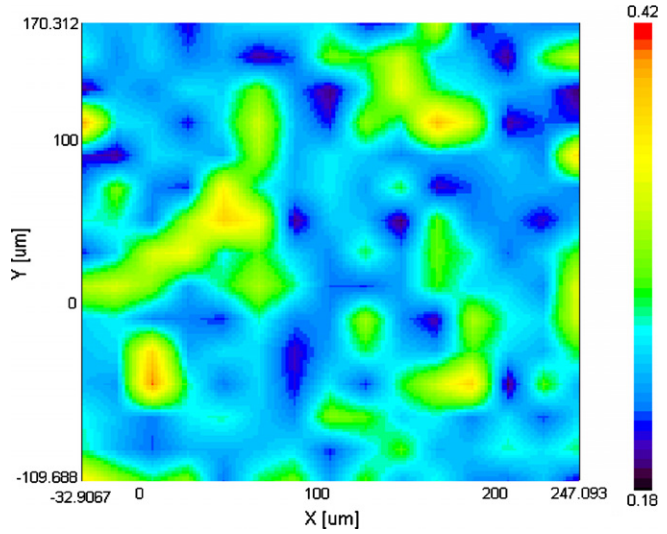

Fig. 4. Raman imaging of a peak height ratio ($Peak_{fiber}/Peak_{matrix}$) of a specimen of PLA with 1 wt% fiber content. The selected matrix peak is at 1122.3 cm^{-1} and fiber peak is at 1090.3 cm^{-1}.

Table 1
DSC melting point and melting enthalpy of the neat films of PHBV and PCL and of their biocomposites with 1, 2, 4, 5, and 10 wt% fiber content prepared by solving casting

Sample	T_m (°C)	ΔH_m (J/g)
PHBV	145–157	47
PHBV+1 wt% fiber	139–154	28
PHBV+5 wt% fiber	137–153	23
PHBV+10 wt% fiber	140–155	37
PCL	62	96
PCL+1 wt% fiber	63	62
PCL+5 wt% fiber	64	69
PCL+10 wt% fiber	62	79

lateral rearrangements and hence crystallization in these two materials.

The thermal behavior of PLA is different and more complex than that of the other two biomaterials, because PLA exhibits (see Fig. 5) a cold crystallization process (Mathew, Oskman, & Sain, 2006) similar to that typically observed for the petroleum-based polyester polyethylene terephthalate (PET). Fig. 4 indicates that the cold crystallization peak occurs at a lower temperature in the biocomposites and it seems to spread over a wider temperature range in composites with 10 wt% fiber. This observation points that, in an opposite effect to that reported above for PCL and PHVB, the fibers can facilitate the crystallization process of the PLA biopolymer. In fact, it has been broadly reported in polypropylene (Quillin, Caulfield, & Koutsky, 1993; Zafeiropoulos, Baillie, & Matthews, 2001; Son, Lee, & Im, 2000; Houshyar & Shanks, 2003; Lenes & Gregersen, 2006) but also in PLA (Mathew et al., 2006) composites, that unmodified cellulose fibers can induce crystal nucleation of these polymers at the fiber surface, i.e. the so-called transcrystallinity effect. The transcrystallinity event is not observable in the optical micrographs here, possibly because the crystallinity of the cast PLA samples is very low (see Table 2). However, the broad single melting peak of PLA is seen to become multiple in the biocomposites, which show two melting peaks with one of them having higher melting point than the neat biopolymer. This latter effect strongly reveals the nucleating role of the fibers, which are able to promote a more robust crystalline morphology for this particular biopolymer during the heating run.

The PLA crystallinity, defined as the area of the melting peak minus the area of the cold crystallization peak, seems somewhat larger, except in the 10 wt% fiber content sample, for the biocomposites than for the neat material indicating that, as mentioned above, the fibers tend to favor some crystallization of the biopolymer (see Table 2). In principle, filler-induced crystallization of the biopolymers is positive from a barrier perspective, since crystals are typically impermeable systems, but crystallization may promote, as a downside, additional rigidity and hence fragility for the biopolymer mechanical performance. Nevertheless, the heat of fusion (crystallinity) is very small for the current cast PLA-based samples compared to the other two biopolymers, indicating that the crystallization process of PLA is extremely metastable. Finally, the polymer T_g was also observed to increase but only in the 1 wt% fiber-PLA biocomposites, highlighting the reinforcing synergetic role of the fibers for this particular composition. The reason for not observing a T_g rise for samples with higher fiber loads could be due to fiber segregation and agglomeration.

In conclusion, the cellulose filler does not have a generic role in the biocomposites thermal properties. Thus, depending on the biomaterial, it has been found to act as impairment to crystal development, as for PCL and PHBV, or as a nucleating agent, as for PLA.

3.3. Mass transport properties

Table 3 gathers all the barrier data (direct permeability, diffusion coefficient and solvent uptake) that has been measured in the neat biopolymers and in their biocomposites and also gathers permeability values reported in the literature for the neat biopolymers.

A curious first observation from Table 3 and regarding PCL is that the water permeability coefficient of 0.4×10^{-13} kg m/s m^2 Pa is much higher than that of 0.0023×10^{-13} kg m/s m^2 Pa previously reported for toluene cast PCL (Messersmith & Giannelis, 1995). The reason for the large disagreement could be related to the different origins of the two samples (lab scale material vs. industrial scale material production) and the fact that molecular weight, the solvent used and the differences in relative humidity gradient used for testing were totally different.

Direct permeability for limonene in PLA was not reported, because the measurements yielded values below the sensibility of the permeation cells; a previous study reported that the limonene permeability for PLA is of ca. 0.000002×10^{-13}kg m/s m^2 Pa when measured at 45 °C

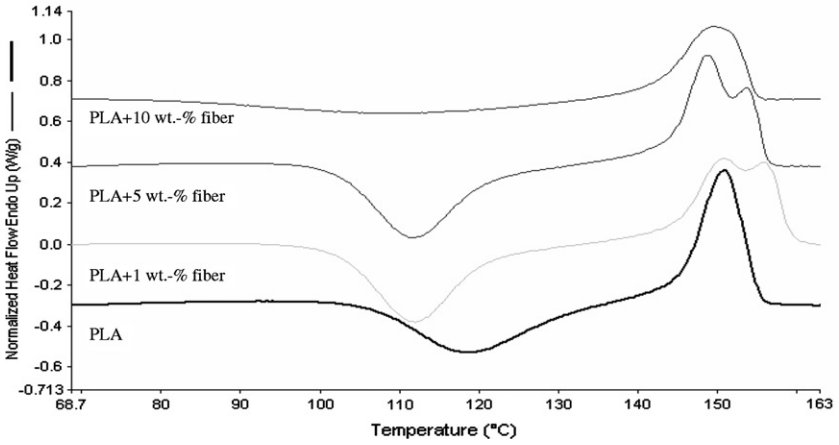

Fig. 5. DSC curves of samples of neat PLA and of their nanobiocomposites with 1, 5, and 10 wt% of the filler.

Table 2
DSC melting point and melting enthalpy of solvent cast PLA and its biocomposites with 1, 5, and 10% wt of filler

Sample	T_m (°C)	T_c (°C)	ΔH_m (J/g)	T_g (°C)
PLA	151	119	3	57
PLA+1 wt% fiber	151–156	112	4	59
PLA+5 wt% fiber	149–154	112	4	56
PLA+10 wt% fiber	150	110	1	55

and 258 Pa of vapor partial pressure gradient (Auras, Harte, & Selke, 2005).

In the case of the PHBV biopolymer, Table 3 and Fig. 6A teach that the limonene and water permeability show minimum values for specimens with 1 wt% fiber content. Further increase in fiber content results in increased permeability to values, as for the case of limonene, even higher than that of the neat component. Films of PHBV with 1 wt% fiber content have a water permeability decrease of 71% compared to the unfilled material, whereas films of PHBV with 10 wt% fiber content show a water permeability reduction of ca. 52%. Increasing fiber content was seen to result in fiber agglomeration and this is thought to cause a reduction in matrix homogeneity and cohesion and lead to preferential penetrant paths and to detrimental effects in barrier properties. A reduction in limonene permeability of ca. 64% and in the diffusion coefficient of ca. 58% is observed in the biocomposite of PHBV with 1 wt% fiber content. Interestingly, limonene uptake appears to remain unmodified, or to increase very slightly, in the biocomposites of this material. However, when the uptake values are corrected for the crystallinity drop of the matrix in the biocomposites (only the amorphous phase is thought to uptake the penetrant), the actual uptake decreases (see corrected uptake values between brackets in Table 3) indicating that the fibers do actually sorb less aroma component than the biopolymer matrix. Thus, the above results suggest that the reduction in permeability for this vapor is both strongly related to a reduction in the diffusion coefficient imposed

Table 3
D-Limonene and water permeability, D-limonene diffusion coefficient and D-limonene % uptake for PHBV and PCL films with 1, 2, 4, 5, and 10 wt% fiber content

	P-limonene (kg m/s m^2 Pa)	P water (kg m/s m^2 Pa)	D-limonene (m^2/s)	Limonene uptake (%)
PHBV	$1.99 \pm 1.01\ e^{-13}$	$0.127 \pm 0.001\ e^{-13}$	$2.21 \pm 0.0\ e^{-13}$	12.7
PHBV+1 wt% fiber	$1.27 \pm 0.08\ e^{-13}$	$0.038 \pm 0.0002\ e^{-13}$	$1.34 \pm 0.09\ e^{-13}$	13.3 (8.1)
PHBV+2 wt% fiber	$1.67 \pm 0.12\ e^{-13}$	$0.049 \pm 0.010\ e^{-13}$	$1.97 \pm 0.73\ e^{-13}$	12.5
PHBV+4 wt% fiber	$1.44 \pm 0.12\ e^{-13}$	$0.093 \pm 0.009\ e^{-13}$	$2.41 \pm 0.63\ e^{-13}$	12.2
PHBV+5 wt% fiber	$1.76 \pm 0.21\ e^{-13}$	$0.053 \pm 0.01\ e^{-13}$	$2.31 \pm 0.1\ e^{-13}$	16.2 (8.1)
PHBV+10 wt% fiber	$2.15 \pm 0.16\ e^{-13}$	$0.067 \pm 0.0005\ e^{-13}$	$2.71 \pm 0.1\ e^{-13}$	15.7 (12.3)
PCL	$5.51 \pm 0.25\ e^{-13}$	$0.339 \pm 0.061\ e^{-13}$	$5.48 \pm 0.0\ e^{-13}$	9.8
PCL+1 wt% fiber	$2.58 \pm 0.56\ e^{-13}$	$0.198 \pm 0.025\ e^{-13}$	$2.86 \pm 0.24\ e^{-13}$	15.3 (9.9)
PCL+2 wt% fiber	$4.96 \pm 0.29\ e^{-13}$	$0.208 \pm 0.005\ e^{-13}$	$4.77 \pm 0.47\ e^{-13}$	14.0
PCL+4 wt% fiber	$3.89 \pm 0.29\ e^{-13}$	$0.252 \pm 0.015\ e^{-13}$	$5.23 \pm 0.82\ e^{-13}$	13.2
PCL+5 wt% fiber	$4.61 \pm 0.16\ e^{-13}$	$0.286 \pm 0.027\ e^{-13}$	$7.30 \pm 0.32\ e^{-13}$	13.2 (9.4)
PCL+10 wt% fiber	$5.28 \pm 0.21\ e^{-13}$	$0.430 \pm 0.013\ e^{-13}$	$7.59 \pm 0.38\ e^{-13}$	14.1 (11.6)
Literature value PCL		[a]$0.0023\ e^{-13}$		

Values between brackets represent uptake values corrected for the heat of fusion (crystallinity) values in Table 1.
[a] (Auras et al., 2005) At 35 °C, 75%RH and cast from toluene.

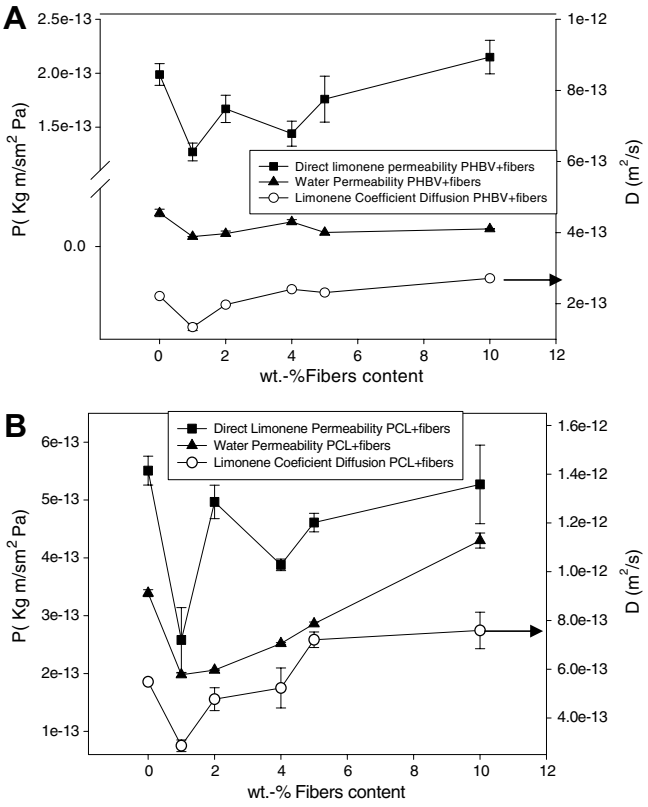

Fig. 6. D-limonene and water direct permeability and limonene diffusion coefficient as determined by gravimetry for (A) the films of PHBV with 1, 2, 4, 5, and 10 wt% fiber contents and (B) the films of PCL with 1, 2, 4, 5, and 10 wt% fiber contents.

by the presence of the fibers but also to a decrease in solubility of the penetrant. It is remarkable to observe that even when the crystallinity of the matrix goes down by the influence of the fibers and, therefore, the matrix should become more permeable, the overall blocking effect of the fiber crystals, well dispersed and embedded in the matrix, overrides this negative effect and drives the biocomposite to become more impermeable.

Fig. 6B and Table 3 show direct limonene and water permeability and limonene diffusion coefficients for films of PCL reinforced with different fiber contents. From the results, a reduction in limonene permeability of ca. 53%, a reduction in water permeability of ca. 58% and in the limonene diffusion coefficient of 52% is observed in the biocomposite with 1 wt% fiber content compared with the unfilled biopolymer. Limonene permeability and diffusion appear to match very well for this material suggesting that the permeability drop could be primarily related to the more tortuous path imposed by the fibers. Limonene uptake (see Table 3) is for the case of neat PCL somewhat lower than for neat PHBV, but the uptake of limonene is higher in the PCL biocomposites. Nevertheless, if a correction for the crystallinity drop of the matrix is carried out the uptake values remain constant pointing that the fibers sorb equally as the matrix. The overall permeability trend

Table 4
Water permeability for PLA films with 1, 4, 5, and 10 wt% fiber contents

	P water (kg m/s m^2 Pa)
PLA	$0.230 \pm 0.007\ e^{-13}$
PLA+1 wt% fiber	$0.208 \pm 0.009\ e^{-13}$
PLA+4 wt% fiber	$0.293 \pm 0.019\ e^{-13}$
PLA+5 wt% fiber	$0.332 \pm 0.027\ e^{-13}$
PLA+10 wt% fiber	$0.414 \pm 0.032E\text{-}^{13}$

is again in agreement with the behavior observed earlier for the PHBV biocomposites.

A curious general observation from Fig. 6 is that while the samples with 1 wt% fiber content show as already mentioned the lowest permeability values, the samples with 2 wt% fiber content tend to increase permeability to values higher than samples with for instance 5 wt% fiber content. This observation may indicate that there must be a balance in the biocomposites between increasing the amount of fiber used, which has in itself barrier capacity, and the permeability deterioration apparently caused by fibber agglomeration. This balance could become less favorable, in the low filler range, for biocomposites with 2 wt% fiber content. The crystallinity drop being higher at low additions of fiber can also add as an effect to account for this observation.

Finally, Table 4 gathers the water permeability of PLA as a function of filler content. These samples indicate that the barrier properties to water of PLA biocomposites is only reduced (by 10%) in the sample containing 1 wt% of fibers. The other composite samples show no barrier improvements and for the case of the 10 wt% fiber content the permeability was seen to increase by ca. 80%. Curiously enough, even when crystallinity (which is for all samples very small) has a potentially favorable impact in most of the biocomposites, except for the case of the 10 wt% sample, the barrier improvement of the very low content biocomposites is smaller than that seen for the other two biomaterials. The reason for this behavior could be attributed to the fact that thicker fiber morphologies where generally observed for the composites of PLA. Thicker fibers imply less dispersed morphologies in the cast material and hence lower tortuosity factors and lower impact in barrier properties.

Acknowledgments

The authors acknowledge the EU integrated project SUSTAINPACK for financial support. NanoBioMatters S.L., Paterna (Spain) and the Spanish MEC Project MAT2006-10261-C03 are also acknowledged for financial support. Finally, M.D.S.G. thank the FPI program of the GV associated to the MEC Project MAT2003-08480-C3 for the research grant.

References

Auras, R., Kale, G., & Singh, S. P. (2006). Degradation of commercial biodegradable packages under real composting and ambient

exposure conditions. *Journal of Polymers and the Environment, 14*(3), 317–334.

Auras, R., Harte, B., & Selke, S. (2005). Sorption of ethyl acetate and D-limonene in poly(lactide) polymers. Society of Chemical Industry. *Journal of the Science of Food and Agriculture*, 0022–5142.

Bodros, E., Pillin, I., Montrelay, N., & Baley, C. (2007). Could biopolymers reinforced by randomly scattered flax fibre be used in structural applications?. *Composite Science Technological 67*(3–4), 462–470.

Colomb, T., Durr, F., Cuche, E., et al. (2005). Polarization microscopy by use of digital holography: application to optical-fiber birefringence measurements. *Applied Optics, 44*(21), 4461–4469.

Crank, J. (1975). *The mathematics of diffusion* (2nd ed.). Oxford: Oxford Science Publications.

Dufresne, A., Dupeyre, D., & Paillet, M. (2003). Lignocellulosic flour-reinforced poly(hydroxybutyrate-co-valerate) composites. *Journal of Applied polymer Science, 87*(8), 1302–1315.

Gross, R. A., & Kalra, B. (2002). Biodegradable polymers for the environment. *Science, 297*, 803–807.

Haugaard, V.K., Udsen, A.M., Mortensen, G., Hoegh, L., Petersen, K. & Monahan, F. (2001). Food biopackaging, in Biobased Packaging Materials for the Food Industry – Status and Perspectives, *Ed. C.J. Weber, Copenhagen*.

Houshyar, S., & Shanks, R. A. (2003). Morphology, thermal and mechanical properties of Poly(propylene) fibre–matrix composites. *Macromolecular Materials and Engineering, 288*, 599–606.

Huang, Z. M., Zhang, Y. Z., & Kotaki, M. (2003). A review on polymer nanofibers by electrospinning and their applications in nanocomposites. *Composites Science and Technology, 63*(15), 2223–2253.

Iannace, S., Luca, N., & Nicolais, L. (1990). Physical characterization of incompatible blends of polymethylmethacrylate and polycaprolactone. *Journal Applied Polymer Science, 41*, 269–2704.

Ichazo, M. N., Albano, C., Gonzalez, J., Perera, R., & Candal, M. V. (2001). Polypropylene/wood flour composites: Treatments and properties. *Composites Structures, 54*, 207–214.

Khalil, H. P. S. A., Shahnaz, S. B. S., Ratnam, M. M., Ahmad, F., & Fuaad, N. (2006). Recycle polypropylene (RPP) wood saw dust (WSD) composites – Part 1: The effect of different filler size and filler loading on mechanical and water absorption properties. *Journal of reinforced plastics and composites, 25*(12), 1291–1303.

Kijchavengkul, T., Auras, R., Rubino, M., Ngouajio, M., & Fernandez, R. T. (2006). Development of an automatic laboratory-scale respirometric system to measure polymer biodegradability. *Polymer Testing, 25*(8), 1006–1016.

Kirby, A. R., Ng, A., Waldron, K. W., et al. (2006). AFM investigations of cellulose fibers in Bintje potato (*Solanum tuberosum* L.) cell wall fragments. *Food Biophysics, 1*(3), 163–167.

Lagaron, J. M., Catalá, R., & Gavara, R. (2004). Structural characteristics defining high barrier polymeric materials. *Materials Science and Technology, 20*, 1–7.

Lenes, M., & Gregersen, W. (2006). Effect of surface chemistry and topography of sulphite fibres on the crystallinity of polypropylene. *Cellulose, 13*, 345–355.

López-Rubio, A., Lagaron, J. M., Ankerfors, M., Lindström, T., Nordqvist, D., Mattozzi, A., et al. (2007). Enhanced film forming and film properties of amylopectin using micro-fibrillated cellulose. *Carbohydrate Polymers, 68*(4), 718–727.

Malainine, M. E., Mahrouz, M., & Dufresne, A. (2004). Lignocellulosic flour from cladodes of Opuntia ficus-indica reinforced poly(propylene) composites. *Macromolecular Material and Engineering, 289*, 855–863.

Mathew, A., Oskman, K., & Sain, M. (2006). The effect of morphology and chemical characteristics of cellulose reinforcements on the crystallinity of polylactic acid. *Journal of Applied Polymer Science, 101*, 300–310.

Messersmith, Pb., & Giannelis, Ep. (1995). Synthesis and barrier properties of poly(ϵ-caprolactone)-layered silicate nanocomposite. *Journal Polymer Science Polymer Chemical, 33*(7), 1047–1057.

Mutje, P., Girones, J., & Lopez, A. (2006). Hemp strands: PP composites by injection molding: Effect of low cost physico-chemical treatments. *Journal Reinforced Plastics Composites, 25*(3), 313–327.

Nabi Sahed, D., & Jog, J. P. (1999). Natural fiber polymer composites: A review. *Advances in Polymer Technology, 18*, 351.

Najafi, S. K., Tajvidi, M., & Chaharmahli, M. (2006). Long-term water uptake behavior of lignocellulosic-high density polyethylene composites. *Journal of Applied Polymer Science, 102*(4), 3907–3911.

Nitz, H., Semke, H., Landers, R., & Mulhaupt, R. (2001). Reactive extrusion of polycaprolactone compounds containing wood flour and lignin. *Journal Applied Polymer Science, 81*, 1972–1984.

Orts, W. J., Shey, J., Imam, S. H., Glenn, G. M., Guttman, M. E., & Revol, J. F. (2005). Application of cellulose microfibrils in polymer nanocomposites. *Journal Polymer Environment, 13*(4), 301–306.

Peoples, O.P. & Sinskey, A.J. (1990). Polyhydroxybutyrate (PHB): a model system for biopolymer engineering: II. *Novel Biodegradable Microbial Polymers* (pp. 191–202). Dordrecht: Kluwer Academic Publishers.

Petersen, K., Nielsen, P. K., Bertelsen, G., Lawther, M., Olsen, M. B., Nilsson, N. H., et al. (1999). Potential of biobased materials for food packaging. *Trends in Food Science and Technology, 10*, 52–68.

Petersson, L., & Oksman, K. (2006). Preparation and properties of biopolymer-based nanocomposite films using microcrystalline cellulose. *American Chemical Society Symposium Series, 938*, 132–150.

PigŁowski, J., & Kiersnowski, A. (2006). Preparation, structure and useful properties of poly(ε-caprolactone)/layered silicates nanocomposites. *Polymers, 51*(10), 704–715.

Quillin, D. T., Caulfield, D. F., & Koutsky, J. A. (1993). Crystallinity in the polypropylene/cellulose system. I. nucleation and crystalline morphology. *Journal of Applied Polymer Science, 50*, 1187–1194.

Rana, A. K., Basak, R. K., Mitra, B. C., Lawther, M., & Banerjee, A. N. (1997). Studies of acetylation, of jute using simplified procedure and its characterization. *Journal Applied Polymer Science, 64*, 1517–1523.

Rosa, D. S., Lotto, N. T., Lopes, D. R., & Guedes, C. G. F. (2004). The use of roughness for evaluating of poly-b-(hidroxybutyrate) and poly-b-(hidroxybutyrate-co-b-valerate). *Polymer Testing, 23*, 3–8.

Son, S.-J., Lee, Y.-M., & Im, S.-S. (2000). Transcrystalline morphology and mechanical properties in polypropylene composites containing cellulose treated with sodium hydroxide and cellulose. *Journal of Materials Science, 35*(22), 5767–5778.

Tserki, V., Matzinos, P., Zafeiropoulos, N. E., & Panayiotou, C. (2006). Development of biodegradable composites with treated and compatibilized lignocellulosic fibers. *Journal of Applied Polymer Science, 100*, 4471–4703.

Zafeiropoulos, N. E., Baillie, C. A., & Matthews, F. L. (2001). Study of transcrystallinity and its effect on the interface in flax fibre reinforced composite materials. *Composites Part A: Applied Science and Manufacturing, 32*(3–4), 525–543.